Supporting Information

for

CO oxidation at nickel centres by N_2O or O_2 to yield a novel hexanuclear carbonate

Bettina Horn, Christian Limberg, Christian Herwig, Michael Feist and Stefan Mebs*

Humboldt-Universität zu Berlin, Institut für Chemie, Brook-Taylor-Str. 2, 12489 Berlin, Germany

* To whom correspondence should be addressed: christian.limberg@chemie.hu-berlin.de

Table of Contents

General Procedures. All manipulations were carried out in a glovebox, or else by means of Schlenk-type techniques involving the use of a dry argon atmosphere. Solvents were purified employing a MBraun Solvent Purification System SPS. The ^{1}H and ^{13}C NMR spectra were recorded on a Bruker DPX 300 NMR spectrometer (^{1}H 300.1 MHz, ^{13}C 75.5 MHz) with dry dmso-d_6 as solvent at 20 °C. The ^{1}H NMR spectra were calibrated against the residual proton, the ^{13}C NMR spectra against natural abundance ^{13}C resonances of the deuterated solvents (dmso-d_6 δ_H 2.50 ppm and δ_C 39.43 ppm). Infrared (IR) spectra were recorded using solid samples prepared as KBr pellets with a Shimadzu FTIR-8400S-spectrometer. Mass spectra (ESI/APCI) were recorded on an Agilent Technologies 6210 Time-of-Flight LC-MS instrument. Microanalyses were performed on a Leco CHNS-932 elemental analyser. The thermal behaviour was studied by simultaneously coupled TA-MS measurements. A NETZSCH thermoanalyzer STA 409 C *Skimmer*®, equipped with a BALZERS QMG 421, was used to record the thermoanalytical curves (T, DTA, TG, DTG) together with the ionic current (IC) curves in the multiple ion detection (MID) mode.[S1,S2] Further experimental details were as follows: DTATG sample carrier system; Pt/PtRh10 thermocouples; platinum crucibles (0.8 mL beaker); sample mass 11-17 mg (measured versus empty reference crucible); constant purge gas flow of 100 mL/min argon 5.0 (AIRLIQUIDE); constant heating rate 10 K/min; raw data evaluation with manufacturer's software PROTEUS® (v. 4.3) and QUADSTAR® 422 (v. 6.02) without further data treatment, e.g. such as smoothing.

Experimental Section – Spectroscopic Details

Synthesis of $K_6[L^{tBu}NiCO_3]_6$, 1, by oxidation with N_2O. A suspension of $K_2[L^{tBu}NiCO]_2$ (80 mg, 63.7 µmol), **I**,[S3] in 5 mL hexane was exposed to an atmosphere of N_2O. The resulting solution was stirred overnight and a brown suspension was formed. All volatiles were removed in vacuo, and the residue was washed with 1 mL tetrahydrofuran. **1** was isolated as a pure light yellow brown powder (45 mg, 11.4 µmol, 54 %). ESI/APCI-MS (250 V, neg, see Figure S5): m/z (%): 619.3441 ($[L^{tBu}NiCO_3]^-$, calc.: 619.3409), 1277.6507 ($K[L^{tBu}NiCO_3]_2^-$, calc.: 1277.6456), 1935.9533 ($K_2[L^{tBu}NiCO_3]_3^-$, calc.: 1935.9503), 2594.2591 ($K_3[L^{tBu}NiCO_3]_4^-$, calc.: 2594.2549), 3252.5626 ($K_4[L^{tBu}NiCO_3]_5^-$, calc.: 3252.5596); IR (KBr): υ = 3170 (w), 3055 (w), 3017 (m), 2959 (vs), 2929 (s), 2908 (s), 2868 (s), 1922 (w), 1858 (w), 1796 (w), 1740 (w), 1623 (vs, CO_3^{2-}), 1614 (vs, CO_3^{2-}), 1533 (m), 1521 (s), 1465 (m), 1445 (m), 1436 (m), 1409 (vs), 1382 (m), 1368 (s), 1322 (vs), 1294 (m, CO_3^{2-}), 1252 (w), 1220 (m), 1208 (w), 1193 (w), 1183 (w), 1164 (m), 1148 (w), 1099 (m), 1055 (m), 1032 (m), 1013 (w), 977 (w), 935 (w), 852 (w), 834 (w), 808 (m), 784 (m), 765 (m), 729 (w), 719 (w), 683 (w) cm^{-1}; ^1H NMR (300.1 MHz, dmso-d_6): δ = 6.83 (m, $^3J_{HH}$ = 7.5 Hz, 2H, Ar-*pH*), 6.72 (m, $^3J_{HH}$ = 7.2 Hz, 4H, Ar-*mH*), 4.98 (s, 1H, C*H*CC(CH$_3$)$_3$), 3.90 (m, $^3J_{HH}$ = 6.8 Hz, 4H, C*H*(CH$_3$)$_2$), 1.74 (d, $^3J_{HH}$ = 6.6 Hz, 12H, CH(C*H*$_3$)$_2$), 1.27 (d, $^3J_{HH}$ = 6.6 Hz, 12H, CH(C*H*$_3$)$_2$), 0.84 (s, 18H, C(C*H*$_3$)$_3$) ppm; $^{13}C\{^1H\}$ NMR (75.5 MHz, dmso-d_6): δ = 164.6 (N*C*C(CH$_3$)$_3$), 164.0 (*C*O$_3$), 145.2 (Ar-*iC*), 142.1 (Ar-*oC*), 123.4 (Ar-*pC*), 121.0 (Ar-*mC*), 96.4 (*C*HCC(CH$_3$)$_3$), 40.6 (*C*(CH$_3$)$_3$), 32.5 (C(*C*H$_3$)$_3$), 27.7 (*C*H(CH$_3$)$_2$), 24.8, 23.1 (CH(*C*H$_3$)$_2$) ppm; Elemental analysis calc. (%) for $C_{216}H_{318}K_6N_{12}Ni_6O_{18}$ (3957.66 g·mol^{-1}): C 65.55, H 8.10, N 4.25; found: C 65.03, H 8.20, N 3.64.

Synthesis of ^{13}1 by oxidation with N_2O. A suspension of $K_2[L^{tBu}Ni^{13}CO]_2$ (60 mg, 47.7 µmol), ^{13}**I**,[S4] in 5 mL hexane was exposed to an atmosphere of N_2O. The resulting solution was stirred over night and a brown suspension was formed. All volatiles were removed in vacuo, and the residue was washed with 1 mL tetrahydrofuran. ^{13}**1** was isolated as a pure light yellow brown powder (37 mg, 9.3 µmol, 59 %). ESI-MS (250 V, neg): m/z (%): 620.3438 ($[L^{tBu}Ni^{13}CO_3]^-$, calc.: 620.3409), 1279.6479 ($K[L^{tBu}Ni^{13}CO_3]_2^-$, calc.: 1279.6456); IR (KBr): υ = 3169 (w), 3056 (w), 3018 (w), 2960 (s), 2930 (m), 2908 (m), 2869 (m), 1923 (w), 1855 (w), 1796 (w), 1617 (w), 1570 (vs, $^{13}CO_3^{2-}$), 1555 (vs, $^{13}CO_3^{2-}$), 1518 (s), 1465 (m), 1445 (m), 1437 (m), 1408 (vs), 1382 (m), 1368 (s), 1321 (s), 1270 (m, $^{13}CO_3^{2-}$), 1253 (m), 1220 (m), 1208 (w), 1193 (w), 1183 (w), 1164 (w), 1148 (w), 1099 (w), 1056 (w), 1031 (w), 977 (w), 935 (w), 808 (m), 784 (m), 765 (m), 718 (w), 683 (w) cm^{-1}; $^{13}C\{^1H\}$ NMR (75.5 MHz, dmso-d_6): δ = 164.0 ($^{13}CO_3$) ppm.

Synthesis of $K_6[L^{tBu}NiCO_3]_6$, 1, by oxidation with O_2. Solid $K_2[L^{tBu}NiCO]_2$ (28 mg, 22.3 µmol), **I**, was treated with neat O_2 for 1 h. Immediately the sample turned light brown. After 12 h at room temperature in contact with O_2 hexane (0.5 mL) was added and the resulting suspension was allowed to ripen for 3 days. The residue was separated from the solution and dried in vacuum to give 8 mg of **1** (2.0 µmol, 27 %).

Employing ^{13}**I** instead of **I** in this reaction leads to the formation of ^{13}**1** as proved by ESI-MS (see Figure S5) and ^{13}C NMR spectroscopy. ESI-MS (250 V, neg): m/z (%): 620.3428 ($[L^{tBu}Ni^{13}CO_3]^-$, calc.: 620.3409), 1279.6495 ($K[L^{tBu}Ni^{13}CO_3]_2^-$, calc.: 1279.6456); 1938.9627 ($K_2[L^{tBu}Ni^{13}CO_3]_3^-$, calc.: 1938.9503); 2598.2756 ($K_3[L^{tBu}Ni^{13}CO_3]_4^-$, calc.: 2598.2549); 3257.5901 ($K_4[L^{tBu}Ni^{13}CO_3]_5^-$, calc.: 3257.5596); $^{13}C\{^1H\}$ NMR (75.5 MHz, dmso-d_6): δ = 164.0 ($^{13}CO_3$) ppm.

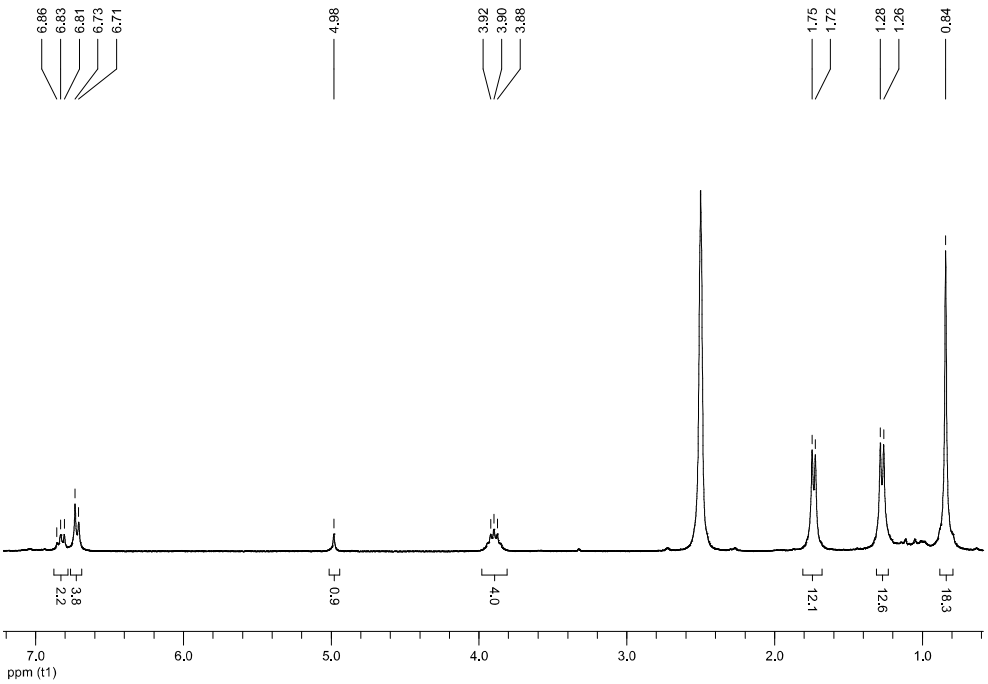

Figure S1. ^{1}H NMR spectrum of $K_6[L^{tBu}NiCO_3]_6$, **1**, dissolved in dmso-d_6.

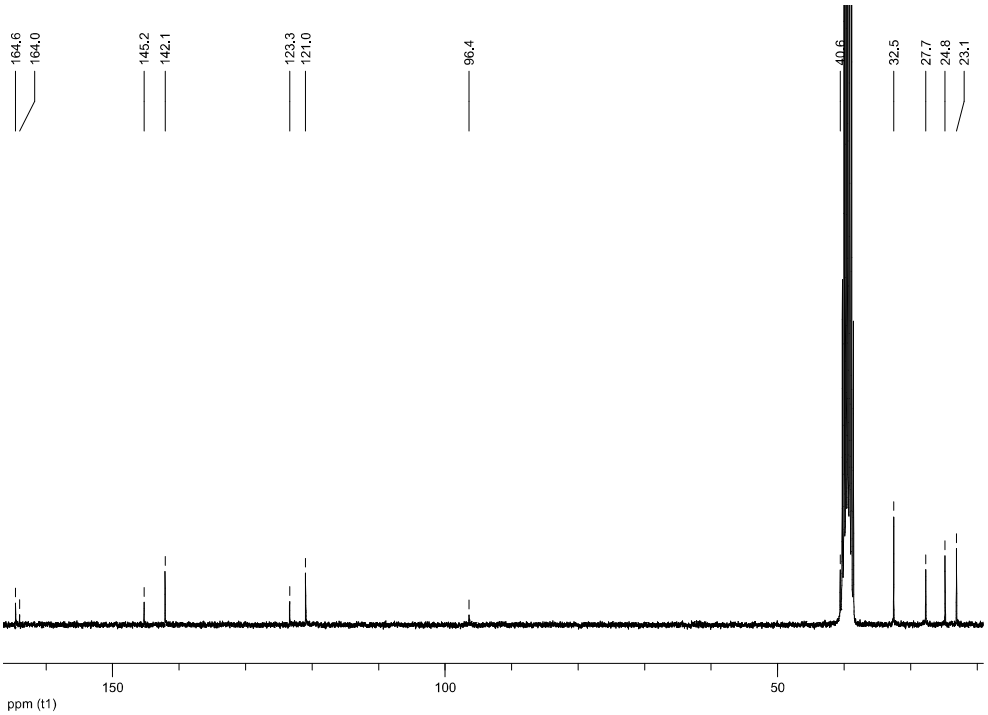

Figure S2. ^{13}C NMR spectrum of $K_6[L^{tBu}NiCO_3]_6$, **1**, dissolved in dmso-d_6.

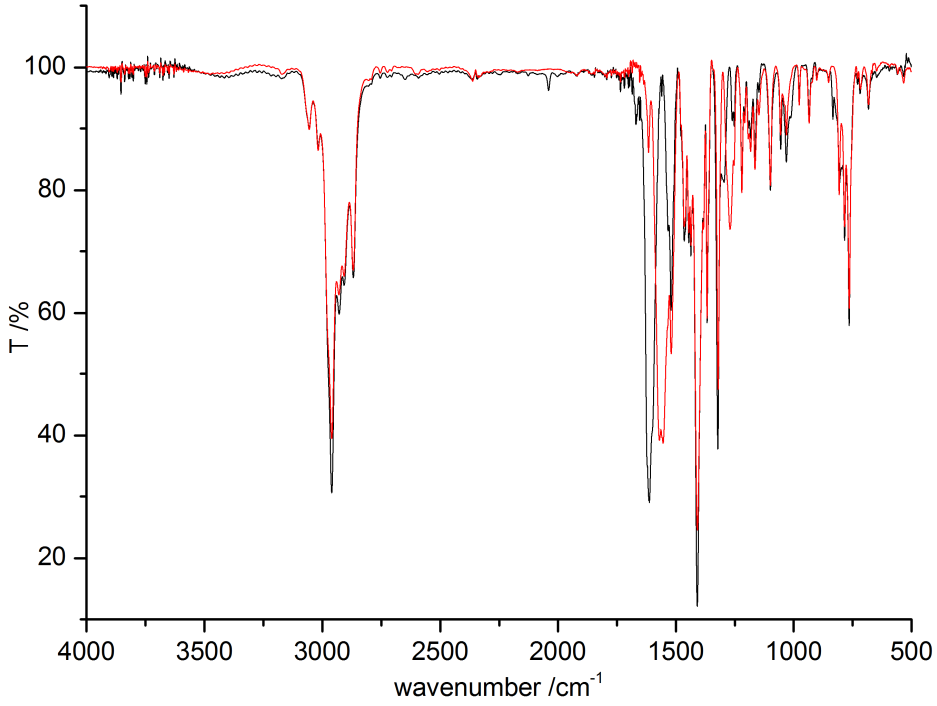

Figure S3. IR spectra of $K_6[L^{tBu}NiCO_3]_6$, **1** (black), and $K_6[L^{tBu}Ni^{13}CO_3]_6$, **^{13}1** (red).

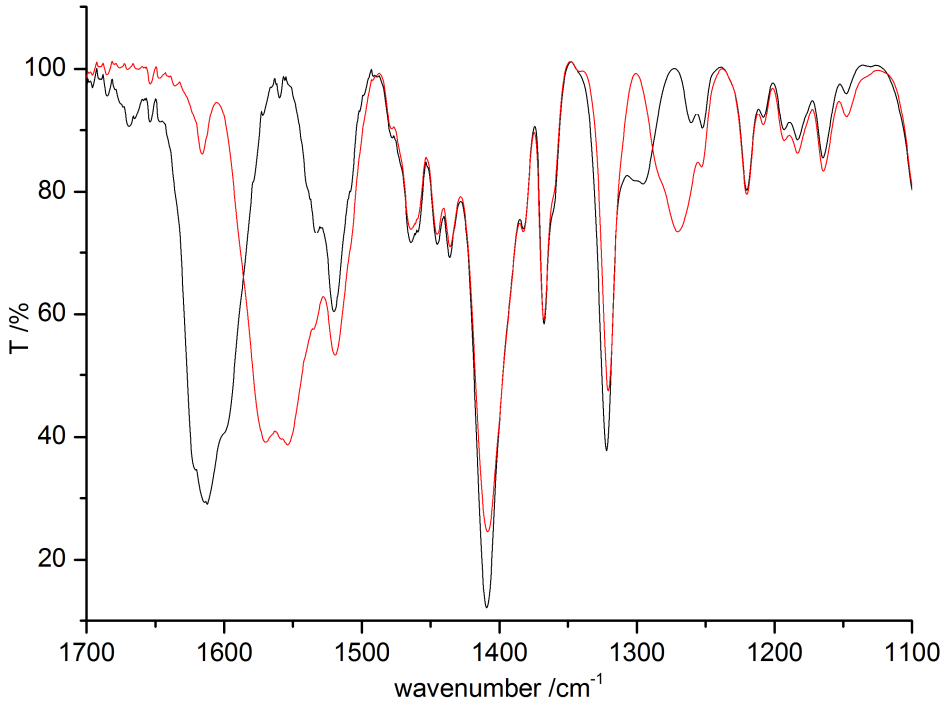

Figure S4. ν_{CO} region of the IR spectra recorded for $K_6[L^{tBu}NiCO_3]_6$, **1** (black), and $K_6[L^{tBu}Ni^{13}CO_3]_6$, **^{13}1** (red).

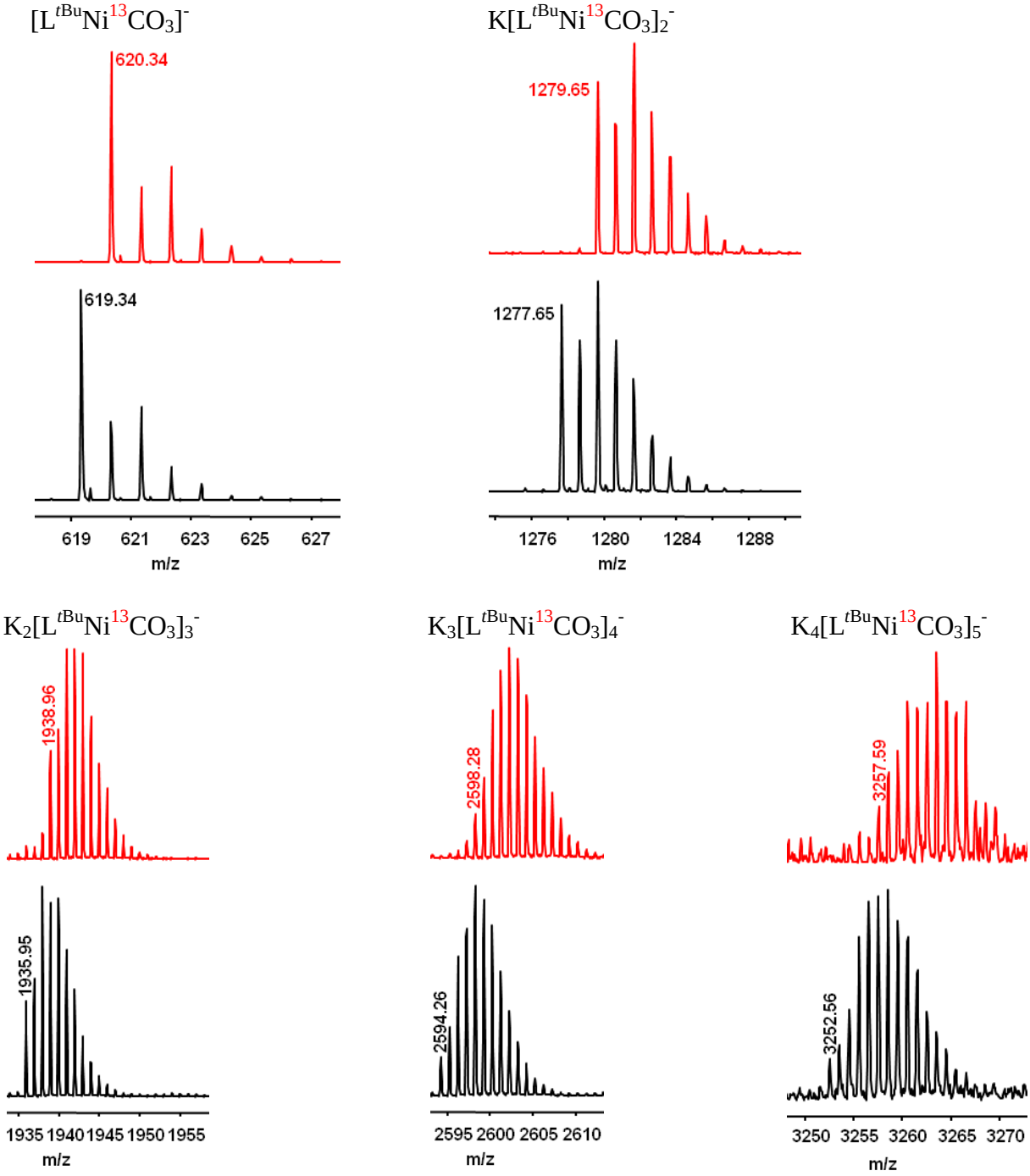

Figure S5. Mass spectra of **1** (ESI/APCI, neg, black) and ^{13}**1** (ESI, neg, red).

Thermal Analysis and *PulseTA*® experiments.

The usual TA-MS curves illustrating the thermal behaviour of the ligand precursor are shown in Figures S6 an S7. The mass numbers m/z = 18 (abbreviated in the following as m18), m44, and m45 are self-explaining in the given context whereas m31 and m57 represent the possible solvent residues methanol and hexane, respectively.

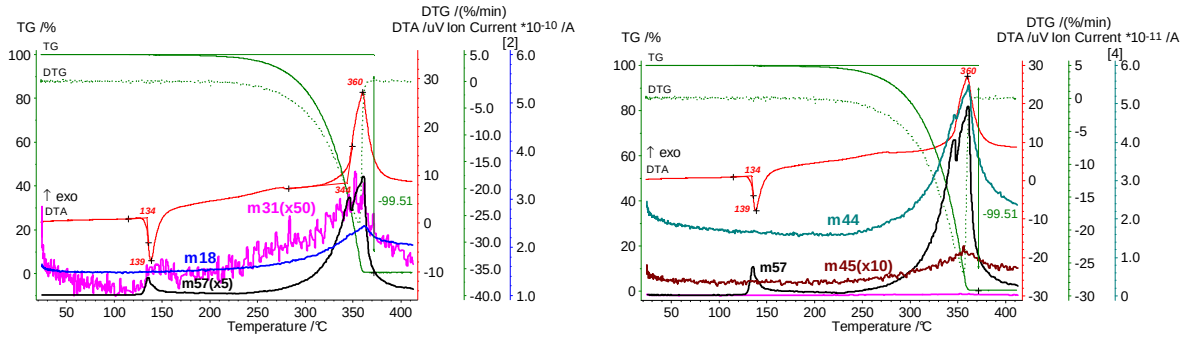

Figure S6 and S7. TA-MS curves of the ligand precursor HL^{tBu} (17.090 mg) in Ar with the IC curves for the mass numbers m/z = 18 (H_2O^+), 31 (CH_3O^+), 44 ($^{12}CO_2^+$), 45 ($^{13}CO_2^+$), and 57 ($C_4H_9^+$).

Figure S8, however, summarizes the essential features of a *PulseTA*® experiment that consists of an internal calibration of the IC signal[S5] representing the molecule expected to be released. The known injected amount is then related to the reaction peak by a simple area comparison of the integral peak areas. The observation that the decomposition of the ligand alone produces the mass number m44 as well (possibly originating from the *i*Pr group, see Figure S7) must not hinder a CO_2 quantification provided one succeeds in separating an additional contribution to the m44 from the basic intensity level of the m44 trace.

The average value of 0.5 µV/s for the calibration peaks in Figure S8 leads to a CO_2 mass of 0.95 mg for the reaction peak which equals to 7.5 equivalents of CO_2 instead of the expected 6 CO_2. This was not satisfying even though the general curve shape of the PTA experiment was excellent. We tried, therefore, to succeed by an evaluation via the mass number m45 ($^{13}CO_2^+$), performed with the labelled compound ^{13}**1**. As only the carbonate carbon was marked in ^{13}**1**, we expected a better distinction of "ligand carbon" from the carbonate carbon, both being responsible for the liberation of CO_2 (cf. Figures S6 and S7).

The corresponding TA run is shown in Figure 9. Here, the injected $^{12}CO_2$ was represented by the mass number m45 ($^{13}CO_2^+$). Accordingly, the IC curve for m45 exhibits an inverted area ratio for calibration and reaction peaks compared with that shown in Figure S8, and the injected volume of 1 mL $^{12}CO_2$ corresponded to 0.0183 mg $^{13}CO_2$ only (cf. the natural isotope ratio ^{12}C : ^{13}C = 100 : 1). With the average value of 0.0081 µV/s one obtains 0.37 mg $^{13}CO_2$ for the reaction peak which equals to 3 equivalents of $^{13}CO_2$ instead of the expected 6 equivalents of $^{13}CO_2$. Again, the quantification is not satisfying. It was found impossible to distinguish between the different contributions to the mass numbers m44 and m45, despite utilisation of the labelled **^{13}1**. This distinction would have been possible exclusively by establishing an *additional* intensity contribution to a given mass number, but the MS sensitivity was obviously too low for it. Note further that the small exothermal effect at ~ 260 °C, preceding the main decomposition step, contributes as well to the total IC signal of m44 and m45 which can be deduced from stronger amplified IC curves (not shown here).

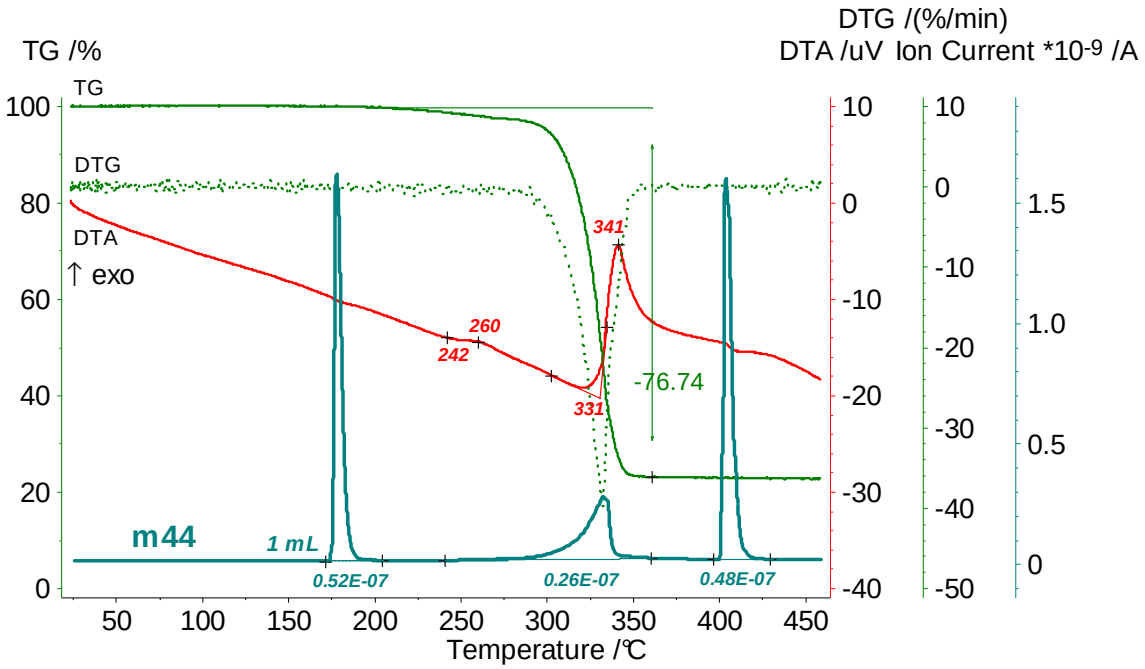

Figure S8. PTA curves of **^{12}1** (11.39 mg) in Ar with the IC curve for m/z = 44 ($^{12}CO_2^+$). Before (170 °C) and after (400 °C) the reaction peak, respectively, 1 mL gaseous $^{12}CO_2$ (1.83 mg CO_2) was injected for calibration.

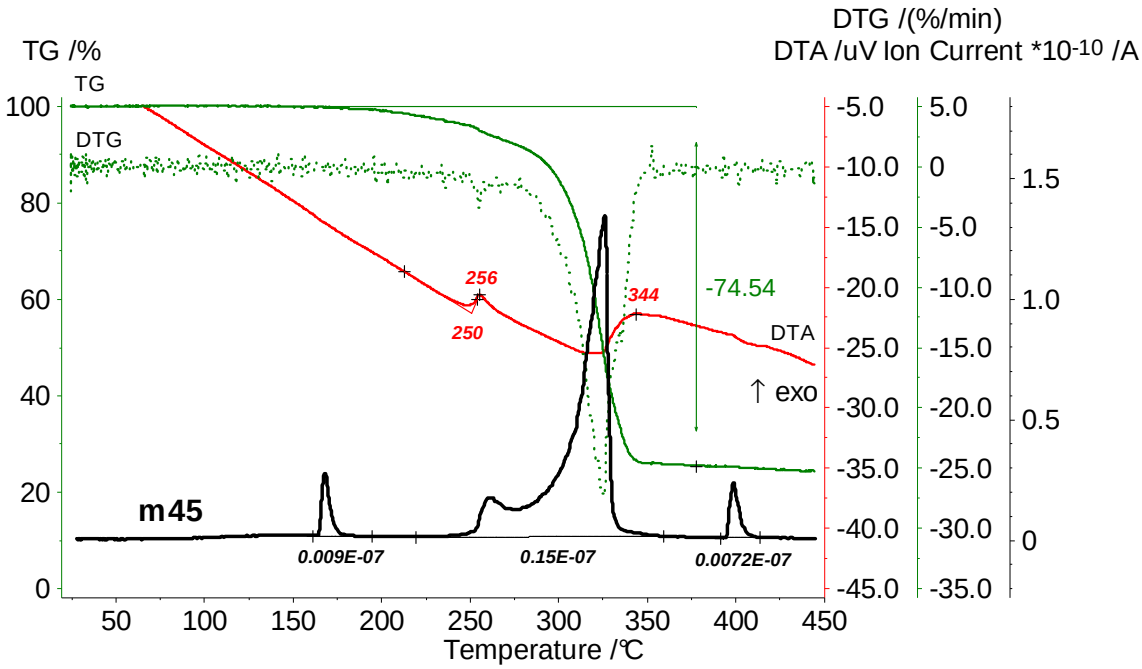

Figure S9. PTA curves of ^{13}**1** (10.62 mg) in Ar with the IC curve for m/z = 45 ($^{13}CO_2$). At 160 °C and 390 °C, respectively, 1 mL $^{12}CO_2$ was injected for calibration (further explanations in the text).

Density Functional Calculations. Geometry optimisations were performed in redundant internal coordinates using the Gaussian09 program package.[S6] The B3LYP functional[S7] was employed together with the Def2-SVP basis set[S8] for C and H atoms and the Def2-TZVPD basis set[S9] for Ni, N, and O atoms, both taken from the EMSL Basis Set Exchange Database[S10]. Very tight convergence criteria were chosen for the SCF procedure and a pruned (99,590) "ultrafine" integration grid was used for numerical integrations. The program NBO5.9[S11] was used for subsequent Natural Bond Orbital (NBO) analysis. Visualisation of molecular structures was accomplished with the program GaussView5.

A cutout of the molecular structure of $K_2[L^{tBu}NiCO]_2$, **I** as determined by X-ray diffraction analysis was used as starting geometry for the mononuclear model $[L^{tBu}Ni(CO)]^-$. The optimised structure is shown in Figure S10 including NBO charges. Both the Ni and the C (carbonyl) atom are positively charged. Due to the relatively small charge differences between these two atoms no clear preference for a nucleophilic attack of N_2O can be derived.

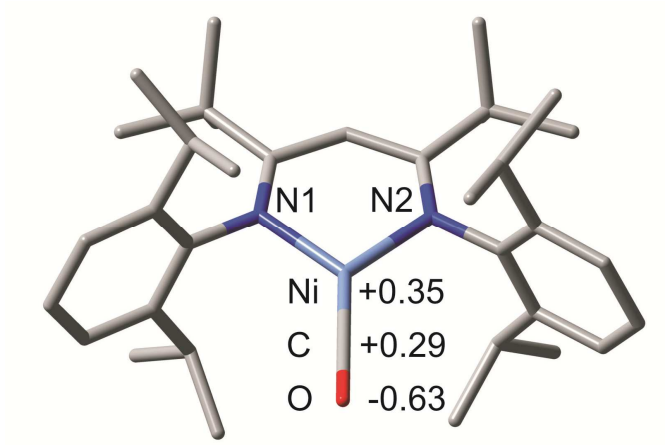

Figure S10. Optimised molecular structure for the singlet state of $[L^{tBu}Ni(CO)]^-$ including NBO charges for selected atoms. Hydrogen atoms are omitted for clarity.

Attempts to optimise the geometry of a $[L^{tBu}Ni(CO)O]^-$ intermediate with different conceivable starting structures always led to the same $[L^{tBu}Ni(\eta^2\text{-}CO_2)]^-$ complex (Figure S11).

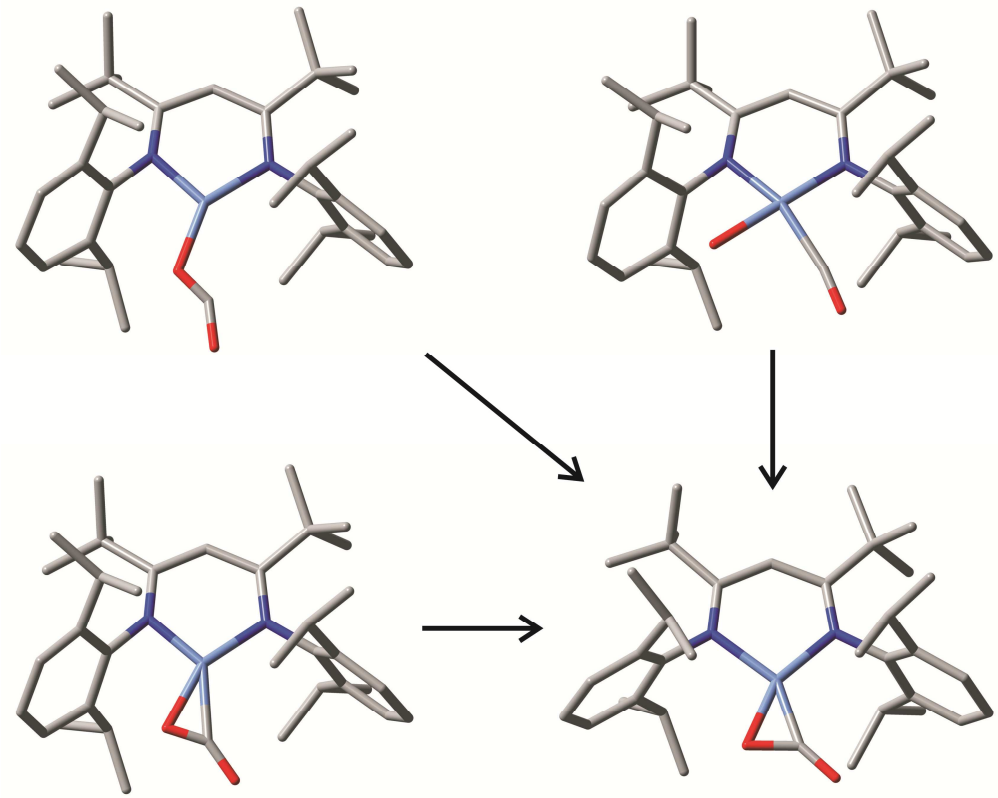

Figure S11. Three different starting structures of an $[L^{tBu}Ni(CO)O]^-$ intermediate leading to the same end structure (bottom right) after optimisation. Hydrogen atoms are omitted for clarity.

Cartesian coordinates (Å) for the theoretical structure of $[L^{tBu}Ni(CO)]^-$, obtained from geometry optimization:

Singlet state, E = –3323.64290754 hartree

	x	y	z
Ni	0.00000000	-1.02741500	0.00009300
N	1.48573800	0.29068300	0.02850000
N	-1.48573900	0.29067900	-0.02855000
O	-0.00000300	-3.91114400	0.00034200
C	-1.97753900	-1.51678000	3.23777100
C	1.30070200	1.60458300	0.03493500
C	2.70876500	-0.41753200	-0.00119000
C	-1.30070300	1.60457700	-0.03521600
C	-2.70876500	-0.41753200	0.00126200
C	-2.68247500	-0.31998600	2.57366600
C	0.00000000	2.17060700	-0.00019000
C	2.43784300	2.70638600	0.09111300
C	3.29011300	-0.90098700	1.20646000
C	3.31973700	-0.73701000	-1.24889200

C	-2.43784300	2.70637000	-0.09158800
C	-3.31974000	-0.73679000	1.24901900
C	-3.29010900	-0.90120100	-1.20630400
C	-3.67156200	0.34184600	3.54841300
C	3.89743800	2.21081900	0.12660600
C	2.24226300	3.55686300	1.37192100
C	2.32608300	3.62135800	-1.15430100
C	4.46758300	-1.65494800	1.14099500
C	2.63052700	-0.65968200	2.56324200
C	4.49380400	-1.49918900	-1.25693000
C	2.68246800	-0.32044200	-2.57361000
C	-2.32609800	3.62154900	1.15367600
C	-3.89743900	2.21079900	-0.12701400
C	-2.24225000	3.55663600	-1.37253400
C	-4.49380800	-1.49896700	1.25718900
C	-4.46758000	-1.65515000	-1.14070900
C	-2.63051900	-0.66013800	-2.56312600
C	5.08234600	-1.95311400	-0.07572600
C	3.54788300	0.07337700	3.55850400
C	2.11630100	-1.97737100	3.17076000
C	3.67155000	0.34121900	-3.54847800
C	1.97753200	-1.51735500	-3.23750100
C	-5.08234600	-1.95310100	0.07606300
C	-2.11628600	-1.97793400	-3.17040400
C	-3.54787300	0.07273900	-3.55852300
C	0.00000000	-2.73662800	0.00024200
H	-1.23446100	-1.95236300	2.55311500
H	-2.70152000	-2.30576700	3.50419400
H	-1.45833600	-1.20641800	4.16127300
H	-1.90328200	0.41997000	2.34181600
H	0.00000000	3.25290800	-0.00028500
H	-3.14346600	0.69847600	4.44924300
H	-4.45077500	-0.36129700	3.88770800
H	-4.18129600	1.20594800	3.09265300
H	4.17878000	1.64523100	-0.76842400
H	4.11235000	1.57661200	0.99342500
H	4.55799100	3.09307800	0.18606700
H	2.30917500	2.92609000	2.27246000
H	1.27015900	4.06755300	1.39818800
H	3.03073200	4.32679600	1.44022700
H	3.12206100	4.38621500	-1.13392700
H	1.36181100	4.14403400	-1.21441500
H	2.44571600	3.03744400	-2.08052000
H	4.91333800	-2.02612300	2.06901000
H	1.75269000	-0.02208200	2.38481900
H	4.95999900	-1.74936100	-2.21456900
H	1.90327400	0.41955300	-2.34188900
H	-1.36182900	4.14424000	1.21371200
H	-2.44573500	3.03778700	2.07999100
H	-3.12208000	4.38639900	1.13317000
H	-4.17878700	1.64535200	0.76810400
H	-4.11234400	1.57645500	-0.99373400
H	-4.55799000	3.09304900	-0.18661800

H	-3.03071900	4.32655700	-1.44097600
H	-2.30915200	2.92571400	-2.27296900
H	-1.27014600	4.06732200	-1.39887500
H	-4.96000500	-1.74897000	2.21487100
H	-4.91333400	-2.02648800	-2.06865900
H	-1.75268500	-0.02250300	-2.38481400
H	6.00195200	-2.54437700	-0.10422200
H	3.89690800	1.03965700	3.16152200
H	4.44155900	-0.52428800	3.80670000
H	3.01396400	0.27184000	4.50378600
H	1.56455800	-1.78798500	4.10762500
H	2.94843100	-2.66349600	3.40414500
H	1.43919400	-2.48758000	2.47051600
H	4.45076300	-0.36198400	-3.88764900
H	4.18128400	1.20540300	-3.09287300
H	3.14345100	0.69768700	-4.44937000
H	1.45832500	-1.20715800	-4.16105600
H	1.23445600	-1.95281900	-2.55276600
H	2.70151400	-2.30638700	-3.50378700
H	-6.00195200	-2.54435800	0.10466200
H	-2.94841300	-2.66410500	-3.40366800
H	-1.43917900	-2.48801400	-2.47006500
H	-1.56454000	-1.78871500	-4.10730100
H	-3.01395100	0.27103100	-4.50383900
H	-3.89690100	1.03909100	-3.16171800
H	-4.44154800	-0.52497200	-3.80661400

References

S1 W.-D. Emmerich, E. Post, *J. Therm. Anal.*, 1997, **49,** 1007.

S2 E. Kaisersberger, E. Post, *Thermochim. Acta*, 1997, **295**, 73.

S3 B. Horn, S. Pfirrmann, C. Limberg, C. Herwig, B. Braun, S. Mebs, R. Metzinger, *Z. Anorg. Allg. Chem.*, 2011, **637**, 1169.

S4 B. Horn, C. Limberg, C. Herwig, S. Mebs, *Angew. Chem.*, 2011, **123**, 12829; *Angew. Chem. Int. Ed.*, 2011, **50**, 12621.

S5 M. Maciejewski, C.A. Müller, R. Tschan, W.-D. Emmerich, A. Baiker, *Thermochim. Acta*, 1997, **295**, 167.

S6 M. J. Frisch, G. W. Trucks, H. B. Schlegel, G. E. Scuseria, M. A. Robb, J. R. Cheeseman, G. Scalmani, V. Barone, B. Mennucci, G. A. Petersson, H. Nakatsuji, M. Caricato, X. Li, H. P. Hratchian, A. F. Izmaylov, J. Bloino, G. Zheng, J. L. Sonnenberg, M. Hada, M. Ehara, K. Toyota, R. Fukuda, J. Hasegawa, M. Ishida, T. Nakajima, Y. Honda, O. Kitao, H. Nakai, T. Vreven, J. A. Montgomery, Jr., J. E. Peralta, F. Ogliaro, M. Bearpark, J. J. Heyd, E. Brothers, K. N. Kudin, V. N. Staroverov, R. Kobayashi, J. Normand, K. Raghavachari, A. Rendell, J. C. Burant, S. S. Iyengar, J. Tomasi, M. Cossi, N. Rega, J. M. Millam, M. Klene, J. E. Knox, J. B. Cross, V. Bakken, C. Adamo, J. Jaramillo, R. Gomperts, R. E. Stratmann, O. Yazyev, A. J. Austin, R. Cammi, C. Pomelli, J. W. Ochterski, R. L. Martin, K. Morokuma, V. G. Zakrzewski, G. A. Voth, P. Salvador, J. J. Dannenberg, S. Dapprich, A. D. Daniels, Ö. Farkas, J. B. Foresman, J. V. Ortiz, J. Cioslowski, and D. J. Fox, *Gaussian 09*, Revision A.02; Gaussian, Inc., Wallingford CT, 2009.

S7 a) A. D. Becke, *Phys. Rev. A*, 1988, **38**, 3098; b) C. Lee, W. Yang, R. G. Parr, *Phys. Rev. B*, 1988, **37**, 785; c) A. D Becke, *J. Chem. Phys.*, 1993, **98**, 5648.

S8 F. Weigend, R. Ahlrichs, *Phys. Chem. Chem. Phys.*, 2005, **7**, 3297.

S9 D. Rappoport, F. Furche, *J. Chem. Phys.*, 2010, **133**, 134105.

S10 a) D. Feller, *J. Comp. Chem.*, 1996, **17**, 1571; b) K. L. Schuchardt, B. T. Didier, T. Elsethagen, L. Sun, V. Gurumoorthi, J. Chase, J. Li, T. L. Windus, *J. Chem. Inf. Model.*, 2007, **47**, 1045.

S11 E. D. Glendening, J. K. Badenhoop, A. E. Reed, J. E. Carpenter, J. A. Bohmann, C. M. Morales, F. Weinhold, Theoretical Chemistry Institute, University of Wisconsin, Madison, WI, 2001; http://www.chem.wisc.edu/~nbo5.